This article has been accepted for publication in a future issue of this journal, but has not been fully edited. Content may change prior to final publication. Citation information: DOI 10.1109/TVT.2016.2605380, IEEE Transactions on Vehicular Technology

Self-tuning of remote electrical tilts based on call traces for coverage and capacity optimization in LTE

V. Buenestado, M. Toril, S. Luna-Ramírez, J.M. Ruiz-Avilés and A. Mendo

***Abstract*—Adjusting antenna tilts is one of the most powerful techniques to solve coverage and capacity problems in cellular networks. In this paper, a novel self-tuning algorithm for adjusting antenna tilts in a LTE system on a cell-by-cell basis is presented. The aim of the algorithm is to improve both network coverage and overall spectral efficiency, while eliminating cell overshooting problems. For this purpose, several new indicators are computed to detect insufficient cell coverage, cell overshooting and abnormal cell overlapping from information available in connection traces. Algorithm assessment is carried out over a static system-level simulator implementing different real macrocellular scenarios. During the analysis, the proposed algorithm is compared with classical self-tuning algorithms that modify other base station parameters, such as transmission power or antenna tilt. Results show that the proposed algorithm can solve overshooting and overlapping problems more effectively than previous algorithms regardless of the scenario.**

***Index Terms*—Mobile network, Long Term Evolution, antenna tilt, optimization, fuzzy logic, call trace.**

I. Introduction

In recent years, the increasing number of users and services in cellular networks has led operators and manufacturers to develop mobile communication systems with greater capacity. In parallel, the complexity of these systems has increased exponentially, making network management a very challenging task. For this reason, operators demand automatic tools for configuring network parameters, as a cheap and flexible solution to improve network capacity without increasing costs.

In this context, operators have identified network Coverage and Capacity Optimization (CCO) as one of the most important use cases of Self-Organizing Network (SON) [1]. The aim of CCO is to provide optimal coverage and capacity, so that network throughput and capacity is maximized while ensuring a certain service confidence level. In second generation systems, such as Global System for Mobile communication (GSM), coverage and capacity issues can be solved independently by frequency planning, so that adjacent cells are allocated different frequencies to avoid co-channel interference. However, in Universal Mobile Telecommunications System (UMTS), coverage and capacity are tightly coupled and have to be treated as a whole. In UMTS, all cells share the same frequency band, which increases cell overlapping and causes large inter-cell interference levels from adjacent cells [2]. To deal with cell overlapping, Wideband Code Division Multiple Access (WCDMA) technology supports macro diversity or soft handover. Likewise, in Long Term Evolution (LTE), all cells use the same frequency band, but no soft handover is included, which makes LTE more sensitive to excessive cell overlapping [3].

Base station antenna tilting is a common technique for improving cell isolation and extending coverage in cellular networks [4]. An optimal tilt configuration minimizes interference from neighbor cells (i.e., overlapping problem), avoids connections with users located far away from the cell (i.e., overshooting problem) and improves coverage in the area that must be served by the base station. Tilting can be achieved mechanically or electrically. The former requires visiting the antenna site and making the changes physically, and it is thus part of long-term network re-planning procedures. Alternatively, antenna tilting can be performed electrically and remotely controlled, which is known as Remote Electrical Tilt (RET). With RET, changing the antenna tilt is as costly as changing any other radio access network parameter. However, there remains the problem of finding the optimum tilt angle settings, as these depend on multiple factors difficult to analyze during network planning and hard to measure during network operation. Such complexity prevents operators from making the most of this technique.

In this work, a novel self-tuning algorithm for modifying antenna tilt values in a LTE system is presented. The proposed algorithm aims to improve the overall network spectral efficiency and eliminate cell overshooting problems by adjusting tilt angles on a per-cell basis. The algorithm is designed as a rule-based expert system implemented by means of a Fuzzy Logic Controller (FLC). The inputs to the algorithm are three new drivers identifying coverage, overshooting and overlapping problems. The term “driver” refers to a low-level indicator used as an input to the algorithm. Unlike previous work, these indicators are computed from connection traces available in the network management system. Algorithm assessment is based on a static system-level simulator implementing two real LTE macrocellular scenarios, consisting of a dense urban and a residential scenario. During the analysis, the proposed algorithm is compared with other self-tuning algorithms inspired in the literature.

The rest of the work is organized as follows. Section II

V. Buenestado, M. Toril and S. Luna-Ramírez are with the Department of Communication Engineering, University of Málaga, 29071, Málaga, Spain e-mail: {vbg, mtoril, sluna}@ic.uma.es.

J.M. Ruiz-Avilés and A. Mendo are with Ericsson, 29590, Málaga Spain e-mail: {jose.maria.ruiz.aviles,adriano.mendo}@ericsson.com.

This article has been accepted for publication in a future issue of this journal, but has not been fully edited. Content may change prior to final publication. Citation information: DOI 10.1109/TVT.2016.2605380, IEEE Transactions on Vehicular Technology

presents the state of research in the CCO problem, justifying the novelty of this work. Section III describes the drivers used to detect overlapping, overshooting and coverage problems, which are the core of the proposed algorithm. Section IV outlines the proposed fuzzy controller for adjusting antenna tilts on a cell basis and two simpler algorithms used later for benchmarking purposes. Section V shows the results of simulations carried out to validate the algorithm. Finally, Section VI discusses several implementation issues and Section VII presents the conclusions.

II. Related work

Several studies have analyzed the influence of antenna tilting in mobile networks. Initial studies cover basic radio aspects in a tilted cell [5][6]. Later simulation studies check the impact of tilting on the overall network performance in different radio access technologies (e.g., GSM [2], UMTS [7][8][9], LTE [10][11]). The analysis is extended to microcellular scenarios in [12][13]. These simulation-based studies are complemented by the field trials in a live GSM network presented in [14][15].

The previous references show the tradeoff between network coverage, quality and capacity when selecting the value of antenna tilt. In the past, antenna tilting was a manual process involving hours of specialized maintenance personnel. Since the cell site had to be switched off for safety reasons during such an adjustment, network operators kept tilt changes to a minimum. Thus, first antenna tilt optimization algorithms were designed as measurement-based replanning procedures, whose aim was to make the most of infrequent tilt changes. For instance, in [15], a method for detecting cells with large overshooting distance based on Timing Advance (TA) statistics is proposed for downtilting antennas in an existing GSM network. Recently, the availability of RET makes it possible to use automatic optimization techniques to find the best tilt settings in large geographical areas periodically. Thus, RET has been proposed by standardization bodies as the main technique for several SON use cases, such as CCO and load balancing [1]. In the literature, many algorithms have been proposed for CCO by RET, which can be classified in self-planning and self-optimization procedures.

Self-planning methods for RET rely on a system model to find the best antenna settings in terms of network coverage, throughput and capacity [16][17][18][19][20]. Once a system model is available, a classical optimization algorithm is used to find the optimum (e.g., geometrical considerations [16][17], brute-force enumeration [19], simulated annealing [18], Taguchi method [20]). These self-planning methods have been used to solve CCO in different radio access technologies, such as WCDMA [18] and LTE [19][20]. Some of them only make use of geometrical considerations [16][17] or consider coverage criteria, such as the ratio of users with Reference Signal Received Power (RSRP) below a certain threshold [19]. Other methods take capacity issues into account by estimating maximum achievable user throughput from average radio link efficiency [20].

In contrast, self-optimization (or self-tuning) methods for RET do not need a system model, but make use of live measurements to adjust tilts following simple control rules. The main limitation of this control-based approach is that there is no guarantee that the optimal tilt settings are found, since no optimization model of the system is used. Due to the difficulty of considering all network performance criteria simultaneously, most methods in this group are conceived as load balancing (or congestion relief) algorithms, and hence control actions are only driven by capacity issues. For instance, the load balancing algorithms for RET described in [21] and [22] do not consider coverage issues. In [23] and [24], a mechanism is added on top of the traffic balance algorithm to ensure adequate network coverage. Only recently, some self-optimization methods for RET have been proposed that also consider network connection quality as a driver. A few of them aim to maximize a single overall performance criterion related to connection quality, such as the average Signal to Interference plus Noise Ratio (SINR) of User Equipments (UEs) [25], average Channel Quality Indicator (CQI) [26], average cell throughput [27] or cell overlapping [28]. Others consider the tradeoff between coverage and connection quality by measuring and comparing cell-edge and cell-center performance in terms of throughput [29], SINR [30][31] or spectral efficiency [32][33]. Alternatively, some methods control the tradeoff between cell overlapping and coverage holes [34][35][36]. In particular, the method proposed in [34] combines a global network entity that ensures overall network coverage by optimizing antenna tilts in a centralized manner, with individual entities in base stations optimizing cell-specific capacity and coverage by tuning pilot power in a distributed manner. While the former is driven by overall network performance measures of coverage and cell overlapping, constructed from RSRP measurements, the latter is driven by cell-specific SINR and RSRP measurements. Likewise, [35] describes a reinforcement learning algorithm to control coverage and connection quality, where coverage issues are detected from RSRP measurements and call dropping and handover failure statistics, while connection quality problems are detected from Reference Signal Received Quality (RSRQ) measurements. Similarly, [36] proposes a rule-based self-tuning algorithm for RET to improve the performance of cell-edge users by detecting coverage holes and excessive cell overlapping from RSRP and SINR measurements, respectively. A similar approach is used in [37], where the tradeoff between coverage and user throughput performance is studied. The latter work is extended in [38] by considering the optimization of both uplink and downlink under sparse system knowledge. In [39], a comparison between online and offline self-optimization of RET is presented, from which it is concluded that simple online methods are preferred when some information is missing.

With a broader scope, some vendors offer automatic tools for detecting cell coverage, overshooting and overlapping problems from drive-test measurements. In these tools, problem detection is performed by comparing the value of some measurable key performance indicator against a pre-defined threshold. For instance, in [40], a methodology for automatic detection of coverage holes, excessive cell overlapping and cell overshooting in UMTS from drive-test measurements is presented. Although these tools are designed for troubleshooting,

This article has been accepted for publication in a future issue of this journal, but has not been fully edited. Content may change prior to final publication. Citation information: DOI 10.1109/TVT.2016.2605380, IEEE Transactions on Vehicular Technology

their output can also be used for RET optimization. However, traditional drive tests carried out with specialized equipment can only cover a very limited geographical area. More recently, the Minimization of Drive Test (MDT) feature [41] can be used to automate measurement collection and thus extend the covered time period and geographical area. With MDT, each UE automatically generates measurement logs at some triggering events, ranging from periodical pilot measurements to detailed radio measurements after a radio link failure. In LTE, the same information can also be extracted from call traces collected by the eNodeB and stored in the network management system.

To the authors' knowledge, no study has considered the use of call traces to optimize RET for extending the coverage area, improving the overall network spectral efficiency and eliminating cell overshooting and excessive overlapping in an existing LTE network. The main contributions of this work are: a) three new indicators used to detect cell overshooting, excessive cell overlapping and poor cell coverage from call traces in the network management system, b) a set of heuristic rules for adjusting tilt angles in a cellular network to increase the coverage area and overall spectral efficiency, while eliminating cell overshooting; and c) a thorough comparison of the proposed algorithm with classical CCO algorithms in realistic scenarios taken from a live network.

III. Drivers

In this section, three indicators for measuring cell overlapping, cell overshooting and cell coverage from call traces are presented. The trace collection process is first introduced and the calculations of the indicators are then explained.

A. Cell and UE traces

The use of real network data is a key tool for improving network optimization algorithms. In mobile networks, network management data is distributed across different elements. Depending on its nature, data can be classified into:

1) Configuration Management (CM) information, reflecting the current value of network parameter settings.
2) Performance Management (PM) information, consisting of counters reflecting the number of times that some event has happened in a network element during a certain period, referred to as Report Output Period (ROP).
3) Data Trace Files (DTF), a.k.a. Performance Recordings, containing multiple records with radio related measurements of a single UE or a base station when some event occurs. There exist different types of DTF, associated to different events (e.g., DTF for failed handovers). DTF can be further classified into User Equipment Traffic Recording (UETR) and Cell Traffic Recording (CTR) [42]. UETR are used to monitor a specific user, while CTR are used to monitor cell performance. Note that both UETR and CTR consist of traces of individual connections. The main difference between UETR and CTR traces is that, in UETR, it is the operator that decides which UE is tracked, whereas, in CTR, all (or a random subset of) UEs in a cell are recorded (i.e., it is not possible to single out a particular user).

The trace collection process starts by the operator preparing the Configuration Trace File (CTF) in the Operations Support System (OSS). The CTF includes: a) the event(s) to be monitored, b) in the case of UETR, the particular UEs, and, in the case of CTR, the cells and the ratio of calls, for which traces are generated, c) the ROP (typically 15 minutes), d) the maximum number of traces activated simultaneously in the OSS, and e) the time period when trace collection is enabled. These parameters must be configured properly to avoid overloading network elements, especially when dealing with high-frequency events (e.g., periodic measurements). After enabling trace collection, UEs transfer their measurement records to their serving eNodeB. When ROP is finished, the eNodeB generates CTR and UETR trace files, which are then sent to the OSS asynchronously. Finally, trace files are parsed and synchronized for their use in network optimization processes.

B. Drivers for antenna tilt optimization

The indicators described in this section are designed to monitor the tradeoff between coverage, quality and capacity in a real LTE network. In interference-limited scenarios, large cell overlapping often leads to better coverage, but worse connection quality and more cell overshooting. This causes that coverage, signal quality and overshooting indicators are usually correlated. However, an excessive cell overlapping does not necessarily leads to a large cell overshooting. For this reason, each indicator must be monitored separately. The novel indicators described next are derived from CTR trace files stored in the network management system.

1) Cell overshooting: Cell overshooting is detected from periodic RSRP measurements in surrounding cells. Overshooting occurs in a cell under study i when a significant share of measurements made by users in very distant cells report a signal level from cell i close to that of the strongest neighbor cell. Those signal levels can be considered as useless cell overlapping, since they do not improve cell coverage (as there already exists a stronger neighbor at those locations), but only increase interference level.

However, it is also common that, at cell edge, two (or more) neighbor cells provide signal levels close to that of the serving cell. This situation is necessary to avoid coverage holes in the transition area between cells. To prevent this situation from being detected as cell overshooting, in this work, neighbor cells are classified into relevant and non-relevant cells. A relevant neighbor is defined as one having a large overlapping area with the source cell. Only measurements in non-relevant neighbors are used to detect cell overshooting.

Specifically, the indicator proposed for measuring cell overshooting of a cell i is the number of non-relevant neighbor cells highly interfered by cell i, $N_{os}(i)$, defined as

$$N_{os}(i) = \sum_{j \in N(i)} (1 - X_{rn}(j,i)) \cdot \min(1, \frac{N_{s_{uon}}(j,i)}{N_s(j) \cdot R_{uon}}), \quad (1)$$

where $N(i)$ is the set of neighbors of cell i; $X_{rn}(j,i)$ is an adjacency-level indicator, explained below, showing whether

This article has been accepted for publication in a future issue of this journal, but has not been fully edited. Content may change prior to final publication. Citation information: DOI 10.1109/TVT.2016.2605380, IEEE Transactions on Vehicular Technology

cell i is a relevant neighbor of cell j (0 means no relevance, 1 means maximum relevance); $N_s(j)$ is the total number of RSRP samples reported by users in cell j; $N_{s_{uon}}(j,i)$ (uon for *useless overlapping* from a *non-relevant* cell) is the number of samples where the RSRP level difference between the serving cell j and neighbor cell i is lower than a pre-defined threshold, $\Delta RSRP_{th_{os}}$, and cell i is not the strongest neighbor; and R_{uon} is a scaling factor between 0 and 1 that defines the ratio of samples needed to consider the source cell i as a strong interferer of adjacent cell j. The $min()$ operator ensures that a neighbor cell j strongly interfered by cell i only adds 1 to $N_{os}(i)$. The parameter $X_{rn}(j,i)$ is defined as

$$X_{rn}(j,i) = \min(1, \frac{N_{s_{rn}}(j,i)}{N_s(j) \cdot R_{rn}}) \,, \tag{2}$$

where $N_{s_{rn}}(j,i)$ (rn for *relevant neighbor*) is the number of samples with RSRP values from neighbor cell i higher than the rest of neighbor, and R_{rn} is the ratio of relevant samples to consider the source cell i as a totally relevant neighbor of adjacent cell j.

2) Useless high-level cell overlapping: Unnecessary high-level cell overlapping is also detected from RSRP measurements in neighbor cells. This occurs when a neighbor cell is received with a RSRP level close to that of the serving cell, when the latter is very high (i.e., low dominance samples close to the serving base station).

Specifically, the indicator proposed for measuring useless cell overlapping generated by cell i is the number of neighbor cells j where a significant share of low dominance samples exists in regions of large RSRP from the serving cell j due to cell i, $N_{ol}(i)$, computed as

$$N_{ol}(i) = \sum_{j \in N(i)} \min(1, \frac{N_{s_{uo}}(j,i)}{N_s(j) \cdot R_{uo}}) \,, \tag{3}$$

where $N_{s_{uo}}(j,i)$ (uo for *useless overlapping*) is the number of samples where RSRP difference between serving cell j and neighbor cell i is lower than a pre-defined threshold, $\Delta RSRP_{th_{ol}}$, and the signal level from the serving cell j is larger than a threshold, $RSRP_{high_{th}}$, and R_{uo} is a scaling factor between 0 and 1 defining the ratio of low dominance samples to consider source cell i as a strong interferer of adjacent cell j. Again, the $min()$ operator ensures that a neighbor with a large area of useless cell overlapping with cell i only adds 1 to $N_{ol}(i)$.

3) Bad coverage: Cell coverage is estimated from RSRP and TA measurements in the source cell. The proposed indicator is designed to detect situations of lack of coverage at cell edge, which can be solved by uptilting the antenna. To measure bad coverage in a cell i, the share of samples with insufficient coverage at cell edge, $R_{bc}(i)$, is defined as

$$R_{bc}(i) = \frac{N_{bcce}(i)}{N_{ce}(i)} \,, \tag{4}$$

where $N_{bcce}(i)$ is the number of RSRP samples below a certain threshold, $RSRP_{low_{th}}$, reported by cell-edge UEs of cell i, and $N_{ce}(i)$ is the total number of samples reported by cell-edge UEs of cell i. In this work, cell edge is the region comprising all distances for which the TA value is beyond the 95$^{\text{th}}$ percentile of the TA distribution of the cell.

IV. Self-tuning algorithm

In this section, a heuristic algorithm to compute tilt changes is presented. The algorithm relies on several assumptions about the influence of tilting the antenna that are discussed below.

A. Assumptions

Antenna tilting has a strong impact on cellular network performance. Large antenna tilt could cause excessively low cell overlapping, which might create a coverage hole. On the other hand, small antenna tilt could lead to excessive cell overlapping, causing large interference to surrounding cells. Likewise, small antenna tilt might cause that the considered cell captures very distant users due to unexpected favorable propagation conditions in small areas that might be covered by another cell. This phenomenon, known as cell overshooting, may lead to handover failures and dropped calls when users move, and it should therefore be avoided. Moreover, a small antenna tilt might enlarge the cell excessively, causing that the cell had capacity problems. Ultimately, the antenna tilt of a base station defines the cell footprint, defining which users are served by each cell, which determines user radio link efficiency.

B. Algorithm structure

The proposed algorithm is designed as an incremental controller that iteratively computes changes in the antenna tilt angle from cell traces. For simplicity, the controller is implemented as a FLC [43]. The main advantage of FLCs, compared to classical Proportional Integrative and Derivative (PID) controllers, comes from the simplicity of defining the behavior of the controller by means of linguistic rules taken from operator previous knowledge.

As shown in Fig. 1, the algorithm consists of two FLCs that work sequentially on a cell-by-cell basis. Each cell executes its two FLCs at the end of each ROP without any coordination with neighbor cells. The inputs to the first FLC are the overshooting indicator, $N_{os}(i)$, and the useless overlapping indicator, $N_{ol}(i)$, described in the previous section. The output is a new variable, $UI(i)$ (for *useless interference*), indicating potential overshooting and overlapping problems, which can be solved by downtilting the antenna. The fuzzy output value, $UI(i)$, quantifies useless interference generated by cell i, and ranges from 0 (no interference) to 1 (large interference). Then, $UI(i)$ is used as an input to the second FLC, together with the bad coverage indicator, $R_{bc}(i)$. The output of the second FLC is the suggested tilt change, $\Delta\alpha(i)$, which may be positive (downtilt) or negative (uptilt).

Both FLCs consist of a fuzzificator, an inference engine and a defuzzificator. The fuzzificator qualifies the FLC inputs with values between 0 and 1 according to the degree of membership of inputs to a qualifying class (e.g., “high” or “low”). Such a mapping is made by membership functions $\mu(N_{os})$ and $\mu(N_{ol})$ in the first FLC, and $\mu(UI)$ and $\mu(R_{bc})$ in the

This article has been accepted for publication in a future issue of this journal, but has not been fully edited. Content may change prior to final publication. Citation information: DOI 10.1109/TVT.2016.2605380, IEEE Transactions on Vehicular Technology

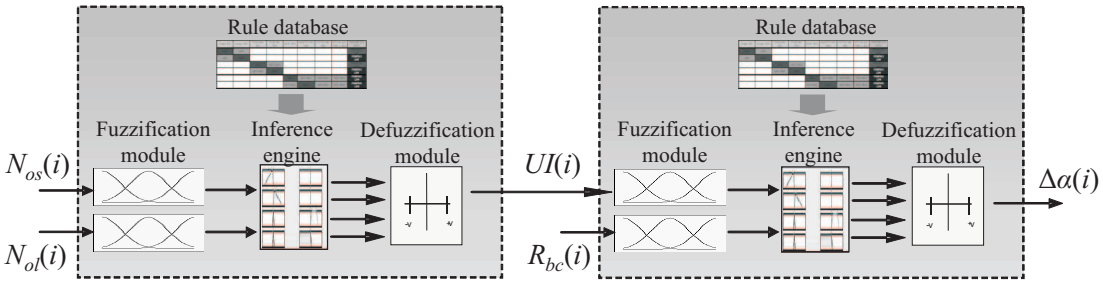

Fig. 1. Diagram of the fuzzy logic controller.

TABLE I
RULES IN THE FIRST FUZZY LOGIC CONTROLLER

No.	$N_{os}(i)$	$N_{ol}(i)$	$UI(i)$
1	Low	Low	Low
2	High	Low	High
3	Low	High	High
4	High	High	High

TABLE II
RULES IN SECOND FUZZY LOGIC CONTROLLER

No.	$UI(i)$	$R_{bc}(i)$	$\Delta\alpha(i)$
1	Low	Low	Equal
2	High	Low	Positive
3	Low	High	Negative
4	High	High	Equal

second FLC. Fig. 2 shows the considered input membership functions, indicating the degree of membership of each value to each class. Note that a certain input value can be qualified simultaneously to different classes due to the overlapping of membership functions.

The inference engine defines the behavior of the controller in linguistic terms by means of "IF ... THEN ..." rules. Unlike classical expert systems, where only one rule is fired at a time, several rules can be fired simultaneously in a FLC. Each rule has its own firing strength depending on the degree in which their antecedents are satisfied. Tables I and II show the rules in the first and second FLC, respectively. For instance, rule 1 in Table I reads as "IF $N_{os}(i)$ (overshooting) is low and $N_{ol}(i)$ (useless overlapping) is low, THEN $UI(i)$ (useless interference) is low". From the rules, it can be deduced that the first FLC detects useless interference when either overshooting or high-level overlapping occurs, whereas the second FLC performs downtilting when useless interference is generated by the cell and uptilting when bad cell-edge coverage exists in the cell.

Finally, the defuzzificator translates the consequent of the rules fired in the inference engine to a numeric value (for the first FLC, the downtilt driver, and, for the second FLC, the suggested parameter change). For this purpose, the center-of-

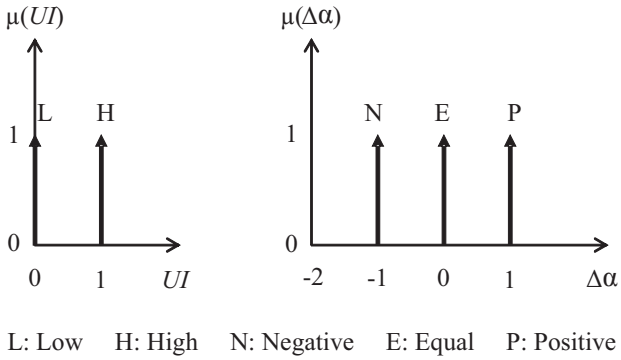

Fig. 3. Output membership functions.

gravity method [43] is used in this work. For simplicity, the controller is designed based on the Takagi-Sugeno approach, where the output membership functions are constant, as shown in Fig. 3. The final output value, $\Delta\alpha(i)$, is rounded to the nearest integer value, so that $\Delta\alpha(i) \in \{-1, 0, 1\}$. Thus, tilt changes are performed in 1-degree steps.

FLC input/output membership functions have been designed to ensure system stability. By firing several rules at a time with different degrees, FLCs achieve a more stable system behavior than conventional rule-based controllers based on threshold crossing. Likewise, the maximum tilt change is limited to 1 degree, avoiding large changes in network performance.

The proposed method works as an iterative process, starting from an initial tilt configuration that is progressively modified. For a certain period of time, referred to as optimization loop, eNodeBs collect CTR traces, from which overshooting, overlapping and coverage indicators are computed. These indicators are used to assess the performance of current antenna tilts on a cell basis. If indicators show performance problems in a cell, a new value for the antenna tilt of this cell is suggested by the FLC. Then, a new optimization loop starts.

The new tilt value is computed by adding the suggested tilt change to the current tilt value. For safety reasons, the final tilt value in cell i is limited to the range [$\alpha_{min}(i)$, $\alpha_{max}(i)$]. α_{max} is set to the maximum tilt angle supported by the vendor equipment. In contrast, α_{min} is used as a geometric brake that takes into account the pointing direction and beamwidth of the antenna. It is considered that an antenna with a tilt value less than its half-power beamwidth, $\theta_{-3\text{dB}}$, radiates much of its energy above the horizon. To avoid this situation, $\alpha_{min}(i)$ =

This article has been accepted for publication in a future issue of this journal, but has not been fully edited. Content may change prior to final publication. Citation information: DOI 10.1109/TVT.2016.2605380, IEEE Transactions on Vehicular Technology

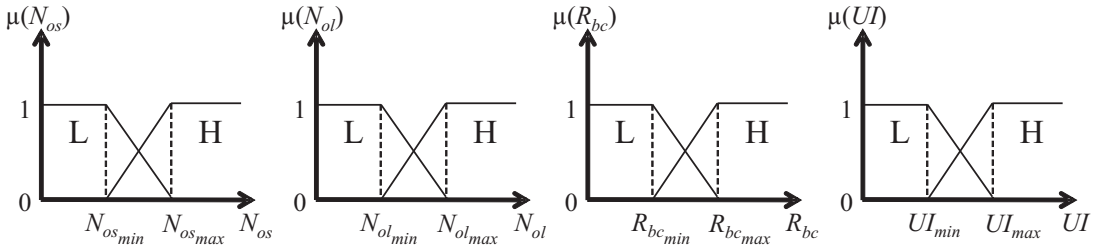

Fig. 2. Input membership functions.

$\theta_{-3\text{dB}}(i)/2$. Note that α_{min}, α_{max} and $\theta_{-3\text{dB}}$ is not necessarily the same in all cells, since the antenna model may be different.

V. Performance assessment

Performance assessment is carried out with a static system-level simulator adjusted with network statistics to reflect a realistic scenario. The assessment methodology is first described and results are presented later.

A. Assessment methodology

This section describes the simulation scenario, the tested self-tuning methods and the network performance indicators used as figures of merit.

1) Simulation scenario: A static system-level LTE simulator has been developed in Matlab. Fig. 4 shows the flowchart of the simulator, following the classical structure of mobile system-level simulators. The analyzed area is divided into a regular grid of points, representing potential user locations. For each network parameter setting (i.e., a tilt plan), received signal level at each point from each base station is computed by a macrocellular propagation model including log-normal slow fading. No fast fading is considered. Then, the serving cell for each point is defined as that providing the maximum signal level. Interference level is estimated by considering a non-uniform spatial user and cell load distribution following a realistic pattern extracted from a live LTE network. Then, connection quality and radio link efficiency are computed. Finally, optimization drivers are calculated by aggregating the previous measurements across all points in the scenario. Only downlink is considered.

In spite of its simplicity, the simulator is designed to make the most of available network statistics to model a live macrocellular scenario. For this purpose, the simulator includes the following features:

i) Delimitation of forbidden areas (i.e., points where users cannot be located) due to water resources by coastline files in Keyhole Markup Language (KML) format.
ii) Parameterization of antenna model on a cell-by-cell basis (e.g., maximum gain, horizontal/vertical beamwidth, ...) depending on vendor equipment.
iii) Initialization of cell load distribution across the scenario with Physical Resource Block (PRB) utilization ratio derived from counters in the network management system of a live LTE network.

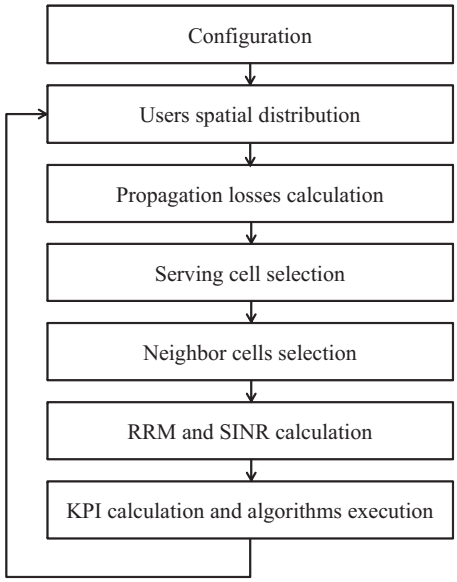

Fig. 4. Simulation flowchart.

iv) Adjustment of spatial user distribution within a cell on an annulus (i.e., distance ring) basis from TA distributions [44].
v) Tuning of propagation model parameters based on the histogram of RSRP measurements.
vi) Update of PRB utilization ratios per cell by estimating the impact of self-tuning algorithms on radio link efficiency of individual users.
vii) Generation of CTR trace files required by self-tuning algorithm, emulating the real trace collection process in the live network.

Two real macrocellular scenarios are implemented in the simulator: a small Inter-Site Distance (ISD) scenario and a large ISD scenario. These might be representative of an interference-limited and coverage-limited scenario. The former is taken from a dense urban area, while the latter is taken from a residential area with small buildings. Table III summarizes the main simulation parameters and some network statistics relevant for the optimization process. The small ISD scenario consists of 129 cells distributed in 44 sites with average ISD of 0.8 km. The large ISD scenario consists of 163 cells distributed in 55 sites with average ISD of 1.1 km. A different propagation model is used to compute Propagation Losses (PL) for each scenario. WINNER II C2 model [45] is used in the small ISD scenario (dense urban area), where user locations are classified

This article has been accepted for publication in a future issue of this journal, but has not been fully edited. Content may change prior to final publication. Citation information: DOI 10.1109/TVT.2016.2605380, IEEE Transactions on Vehicular Technology

into Line Of Sight (LOS) or Non-Line of Sight (NLOS) conditions based on geolocated data of buildings and antenna position. The variable X in Table III is an environment-specific term included in this model for adjusting NLOS-users propagation losses from network statistics [45]. In the large ISD scenario (residential area), the COST-231 model [46] is used. Model constants are adjusted with RSRP statistics from each area. The impact of antenna tilt is modeled by changing the antenna gain in the horizontal and vertical planes. Although these models do not take into account local phenomena, such as reflections or bending, it has been checked on the field that the overall effect of tilting the antenna is modeled correctly in both scenarios. The rest of parameters are directly taken from the real network. Both scenarios include a single carrier at 734 MHz with 10 MHz system bandwidth (i.e., 50 PRBs). Resolution in TA measurements is 40 m. Antenna tilt/height and transmit power settings differ among cells. Traffic and PRB utilization data is taken from the busy hour.

2) Tested algorithms: Four planning methods are compared in this work. A first method is the tilt plan implemented by the operator, denoted as OS (Operator Solution). OS is the baseline against which all other methods are compared. This plan is expected to show excessively low tilt angles, as tilt configuration is often set when the site is first launched, and remains unchanged when new sites are deployed in the surroundings, generating useless cell overlapping.

A second method is the iterative self-tuning algorithm for RET based on CTR trace files described in Section IV, which is denoted as TF-RET (for Trace-based Fuzzy). This method is initialized with the OS tilt plan and 20 iterations (optimization loops) are simulated. It is checked a posteriori that this number of iterations is enough to reach equilibrium. For brevity, the analysis is restricted to the solution obtained in the last iteration. Table IV presents internal parameter settings in TF-RET. From the table, it is deduced that internal settings are defined so that: a) cells interfering more than one non-relevant neighbor cell, or having useless high-level overlap with more than two neighbors, are candidates for downtilting, and b) cells with more than 20% of RSRP measurements at cell edge below -105 dBm are candidates for uptilting. These settings are used for both scenarios and have been set from a field trial carried out on a very large geographic area that covers different network topologies. Such settings should therefore be valid for any network scenario.

A third method is a variant of the TF-RET method, where the same rules are used to adjust base station transmit power, P_{tx}, instead of antenna tilt. This method, denoted as TF-PWR (for PoWeR), is a backup solution for sites where RET is not available or RET is shared by antennas of different technologies. The output of TF-PWR is the suggested transmit power change, ΔP_{tx}. This method is initialized with the maximum transmit power, which is then reduced to eliminate unnecessary cell overlapping using the rules in TF-RET. As in TF-RET, 20 iterations of TF-PWR are simulated.

A fourth method is the simple formula for adjusting tilt angles based on geometric considerations proposed in [16][17], denoted here as G-RET (for Geometric). In G-RET, the optimum antenna tilt angle for a cell i, $\alpha_{geo}(i)$, is that ensuring

TABLE IV
TF-RET PARAMETER SETTINGS

	FLC 1	
N_{os}	$\Delta RSRP_{th_{os}}$ [dB]	6
	R_{uon} [%]	5
	R_{rn} [%]	10
	$N_{os_{min}}$	0.9
	$N_{os_{max}}$	1
N_{ol}	$\Delta RSRP_{th_{ol}}$ [dB]	6
	R_{uo} [%]	5
	$RSRP_{high_{th}}$ [dBm]	-80
	$N_{ol_{min}}$	1.95
	$N_{ol_{max}}$	2.05
	FLC 2	
R_{bc}	$RSRP_{low_{th}}$ [dBm]	-105
	$R_{bc_{min}}$	15
	$R_{bc_{max}}$	20
UI	UI_{min}	0
	UI_{max}	1

that the vertical antenna gain in the direction of the cell edge is 3 dB below the maximum value, i.e.,

$$\alpha_{geo}(i) = \alpha_{ce}(i) + \frac{\theta_{vert}^{BW}}{2}(i)\,, \tag{5}$$

where $\alpha_{ce}(i)$ is the angle subtended by the antenna structure from a user located at the edge of cell i and θ_{vert}^{BW} is the 3 dB vertical beamwidth. The angle $\alpha_{ce}(i)$ is computed as [17]

$$\alpha_{ce}(i) = \arctan\,\frac{h_{BS}(i) - h_{MS}}{r(i)}\,, \tag{6}$$

where $h_{BS}(i)$ and h_{MS} are the base station and mobile station heights, respectively, and $r(i)$ is the cell radius. Cell radius is estimated from cell edge points. Cell edge points are obtained geometrically by Voronoi tessellation. Cell radius is computed as the average distance from cell edge points to the site location. To extend the analysis, G-RET is tested with different configurations of vertical gain losses at cell edge. For this purpose, θ_{vert}^{BW} parameter is computed for values of vertical gain loss at cell edge other than 3 dB. Nonetheless, the suggested 3 dB value is used as the default G-RET configuration when compared to other algorithms.

Both TF-RET and TF-PWR use RSRP and TA measurements from CTR traces. In the simulation tool, RSRP and TA distributions are generated by processing propagation matrices and distance information, respectively.

3) Key network performance metrics: Two figures of merit are used to assess algorithms:

- the overall average DL SINR, $\overline{SINR_{avg}}$, calculated as the arithmetic mean across the scenario of the average DL SINR per cell, as a measure of network connection quality and spectral efficiency, and
- the overall cell-edge DL SINR, $\overline{SINR_{ce}}$, calculated as the arithmetic mean across the scenario of the 5th-percentile of DL SINR per cell, as a measure of network coverage.

This article has been accepted for publication in a future issue of this journal, but has not been fully edited. Content may change prior to final publication. Citation information: DOI 10.1109/TVT.2016.2605380, IEEE Transactions on Vehicular Technology

TABLE III
SIMULATION PARAMETERS AND NETWORK STATISTICS

Simulation parameters		
Propagation model [dB]	Small ISD	Winner II C2 [45] with X=14 for NLOS users
	Large ISD	$PL = 152.7 - 13.82 \log_{10}(h_{BS}[\text{m}]) +$
		$+(64.37 - 6.55 \log_{10}(h_{BS}[\text{m}])) \log_{10}(d[\text{km}])$
Spatial traffic distribution		Based on TA measurements
Grid resolution [m]		40
Network characteristics		
Carrier frequency [MHz]		734
System bandwidth [MHz]		10
Number of PRBs		50
Maximum allowed tilt [^{o}]		16
UE height [m]		1.5
eNodeB transmit power [dBm]		[46.5, 47.4]
Maximum antenna gain [dB]		15
Antenna 3-dB vertical beamwidth [^{o}]		9.5, 12, 15
	Small ISD	Large ISD
Number of sites	44	55
Number of cells	129	163
PRB utilization ratio [%]	[5, 70]	[5, 60]
Avg. PRB utilization ratio [%]	24	29
Initial antenna tilt angle [^{o}]	[0,13]	[1,14]
Antenna height [m]	[3, 54]	[10, 45]
Avg. inter-site distance [m]	815	1110

Both SINR indicators are computed in the same set of locations (i.e., users) in all iterations. In a first iteration with the initial tilt settings, the set of locations with enough signal level from their serving cell is identified. In subsequent iterations, the set of locations is kept the same, regardless of their signal level/quality. Such a decision aims to ease the comparison of different tilt configurations ensuring that the geographical area where they are compared is exactly the same.

B. Results

The analysis is first focused on the small and large ISD scenarios with the real traffic distribution. Then, the impact of network load is investigated.

1) Small ISD scenario: Fig. 5 presents the results obtained by RET algorithms in the dense urban scenario. Overall cell-edge and cell-average SINR metrics are shown on the x- and y-axis, respectively. Network parameter plans in the upper right part of the figure show better performance. OS planning method (used as reference) is represented by a single dot (diamond). In contrast, iterative methods (i.e., TF-RET and TF-PWR) are represented by a curve of multiple dots showing the performance of intermediate network parameters settings reached across iterations. For clarity, the last value in iterative methods is highlighted with a filled marker. Note that both TF-RET and TF-PWR curves start with the OS network configuration, and their performance is thus the same in the first iteration. The curve for the G-RET planning method represents different values of vertical gain losses at cell edge from 0 to 6 dB in 1-dB steps. Recall that the 3 dB value corresponds to the classical G-RET method, which is used unless otherwise stated.

In Fig. 5, it is observed that the proposed TF-RET algorithm improves both average and cell-edge SINR performance of OS more than the rest of methods. Specifically, $\overline{SINR_{avg}}$ is improved by 1.01 dB and $\overline{SINR_{ce}}$ is increased by 1.14 dB. Table V compares the performance of the iterative methods TF-RET and TF-PWR at the end of the optimization process against that of the operator solution OS and the classical geometrical method G-RET. Again note that the OS row is the starting point for TF-RET and TF-PWR algorithms. Table V also presents the overall average and cell-edge DL user throughput, $\overline{UeTHP_{avg}}$ and $\overline{UeTHP_{ce}}$ respectively, calculated as the arithmetic mean of the individual cell values (average and cell-edge DL user throughput, respectively). DL user throughput in each user location is computed from SINR values by the bounded Shannon formula [47], assuming that the whole system bandwidth is available to the user. First, it is observed that most methods outperform the current operator solution. It is also observed that TF-RET outperforms other optimization approaches, since it achieves the best overall cell-edge SINR for the same overall average SINR. The same trend

This article has been accepted for publication in a future issue of this journal, but has not been fully edited. Content may change prior to final publication. Citation information: DOI 10.1109/TVT.2016.2605380, IEEE Transactions on Vehicular Technology

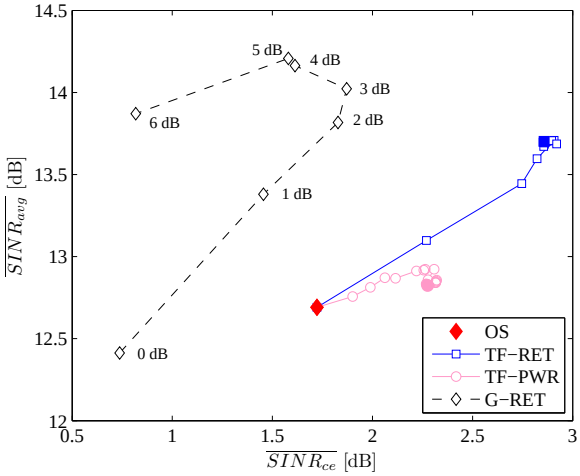

Fig. 5. Performance comparison in small ISD scenario.

is observed for $\overline{UeTHP_{avg}}$ and $\overline{UeTHP_{ce}}$ indicators, for which TF-RET reaches the best values.

In the figure, it is seen that some G-RET configurations obtain slightly better $\overline{SINR_{avg}}$, but much worse $\overline{SINR_{ce}}$ values.

To explain the superiority of TF-RET, a closer analysis of low-level indicators is done. Table VI presents the average values at the end of the optimization process of several indicators used by the algorithms, including the overall average RSRP, $\overline{RSRP}$, and the overall average DL interference, $\overline{I_{DL}}$, computed both as the arithmetic mean of the averages per cell across the scenario. Again note that the OS column in the table is the starting point for TF-RET and TF-PWR. Recall that TF-RET only performs downtilting in cells generating overshooting and/or useless overlapping, and not experiencing cell-edge coverage problems. These downtilt actions made to improve surrounding cells also improve the average received signal level in the source cell (as the antenna is redirected to the center of the cell) without deteriorating its cell-edge performance excessively (since the cell is checked not to have problems at cell edge). At the same time, TF-RET only performs uptilting in those cells with bad cell-edge performance that do not generate overshooting and/or useless overlapping. The combination of both actions should lead to an improvement of network coverage without deteriorating connection quality. This is confirmed by the fact that TF-RET is the only method that manages to reduce bad coverage ratio without increasing interference levels. Specifically, $\overline{R_{bc}}$ is decreased by 3.57% in absolute terms (i.e., from 32.45% to 28.88%), while $\overline{I_{DL}}$ is decreased by 0.75 dB (i.e., from -101.13 to -101.88 dBm).

Alternatively, TF-PWR decreases transmit power in cells generating overshooting and/or useless overlapping that do not experience cell-edge coverage problems. In the table, it is observed that the average transmit power in the scenario can be decreased considerably (i.e., by 1.55 dB) without affecting the overall network performance. However, unlike TF-RET, TF-PWR negatively affects both cell-center and cell-edge users in the source cell whose power is reduced. Thus, the tradeoff between the performance of the source cell and that of the surrounding cells is more evident with TF-PWR. This limitation causes that the bad coverage ratio in the source cell has to be increased to decrease cell overshooting and interference in neighbor cells. Specifically, with TF-PWR, $\overline{I_{DL}}$, that is the overall average DL interference calculated as the arithmetic mean across the scenario of the average DL interference per cell, is decreased by 1.24 dB, but $\overline{R_{bc}}$ is increased by 2.32% in absolute terms, when compared to OS. As a result, the general SINR improvement from TF-PWR is not as large as with TF-RET, as shown in Table V.

TABLE VI
LOW-LEVEL INDICATORS AT THE END OF THE OPTIMIZATION PROCESS IN SMALL ISD SCENARIOS

	OS	TF-RET	TF-PWR	G-RET (3 dB)
$\overline{N_{os}}$	1.18	0.81	0.93	0.91
$\overline{N_{ol}}$	1.00	0.95	1.02	0.98
$\overline{R_{bc}}$ [%]	32.45	28.88	34.77	33.74
$\overline{RSRP}$ [dBm]	-88.44	-88.17	-89.55	-88.24
$\overline{I_{DL}}$ [dBm]	-101.13	-101.88	-102.37	-102.26
$\overline{\alpha} - \overline{\alpha_{\text{OS}}}$ [^{o}]	0	0.50	0	1.65
$\overline{P_{tx}} - \overline{P_{tx_{\text{OS}}}}$ [dB]	0	0	-1.55	0

Unlike TF-RET and TF-PWR, G-RET performs tilt actions based on geometric cell edge, without taking the irregular spatial user distribution into account. In Fig. 5, three different regions are observed for G-RET:

1) When the vertical gain loss at cell edge is set to 0 dB, every antenna is pointed to the geometric cell radius. Thus, users located close to the base station receive lower power levels, leading to lower $\overline{SINR_{avg}}$ values. Moreover, the interference generated in neighbor cells is greater. As a result, both spectral efficiency and coverage figures of merit decrease.
2) When the vertical gain loss at cell edge is increased (i.e., 1, 2 or 3 dB), antennas point closer to base stations. Then, cell-centre users are better covered and interference generated in neighbor cells is lower. As a result, both $\overline{SINR_{avg}}$ and $\overline{SINR_{ce}}$ improve.
3) Finally, when the vertical gain loss is set to larger values (i.e., 4, 5 or 6 dB), antennas are excessively downtilted, causing that users located far from base stations do not receive enough power, even if users located closer receive better signal and the interference generated in neighbor cells is lower. Thus, $\overline{SINR_{avg}}$ improves, but $\overline{SINR_{ce}}$ decrease.

In practice, G-RET tends to give downtilt values larger than TF-RET, as G-RET is based on geometric considerations and does not take into account that a significant share of users are beyond the geometric radius (e.g., due to slow fading or handover margins). In this scenario, the average deviation from the initial tilt angle in OS is 1.65^o with the classical G-RET and 0.50^o with TF-RET. As a result, $\overline{R_{bc}}$ with G-RET is

This article has been accepted for publication in a future issue of this journal, but has not been fully edited. Content may change prior to final publication. Citation information: DOI 10.1109/TVT.2016.2605380, IEEE Transactions on Vehicular Technology

TABLE V
METHOD PERFORMANCE IN SMALL ISD SCENARIO

	$\overline{SINR_{avg}}$ [dB]	$\overline{SINR_{ce}}$ [dB]	$\overline{UeTHP_{avg}}$ [Mbps]	$\overline{UeTHP_{ce}}$ [Mbps]
OS	12.69	1.72	25.96	8.27
TF-RET	13.70	2.86	27.80	9.67
TF-PWR	12.82	2.28	26.18	8.92
G-RET (3 dB)	14.02	1.87	28.46	8.84

significantly larger (i.e., 33.74%) when compared to than with TF-RET (i.e., 28.88%). This is the main reason for the lower SINR cell-edge performance of G-RET observed in Figure 5 and Table V.

2) Large ISD scenario: Fig. 6 and Table VII show the performance of the different algorithms in the residential scenario. Again, TF-RET achieves the best average SINR and user throughput values. However, performance gain is lower in this scenario (coverage-limited) compared to the one with small ISD (interference-limited). Specifically, $\overline{SINR_{avg}}$ and $\overline{SINR_{ce}}$ are improved by 0.44 and 0.37 dB, respectively, in this scenario (against 1.01 and 1.14 dB in the small ISD scenario). Likewise, $\overline{UeTHP_{avg}}$ and $\overline{UeTHP_{ce}}$ are improved by 0.83 and 0.49 Mbps, respectively, in this scenario (against 1.84 and 1.40 Mbps in the small ISD scenario). Unlike TF-RET, TF-PWR hardly performs any change in the network configuration. A closer analysis (not presented here) shows that most cells in this scenario suffer from bad cell-edge performance because of the large cell radius (i.e., 1.1 km on average). As a consequence, TF-PWR keeps the transmit power to the initial (i.e., maximum) value for most cells. The solutions thus obtained by TF-PWR are nearly the same across iterations, which is the reason why all points in the TF-PWR curve in Fig. 6 are on top of each other. Likewise, TF-RET outperforms the classical version of G-RET in terms of $\overline{SINR_{avg}}$ and $\overline{SINR_{ce}}$ by 0.18 and 0.38 dB, respectively. It should be pointed out that, in this case, the best results in G-RET are obtained for 1 dB vertical losses (instead of the typical configuration of 3 dB).

3) Impact of network load: Fig. 7 and Table VIII show the result obtained from the proposed optimization algorithm when the network is highly loaded. For this purpose, OS and TF-RET are evaluated in the small ISD scenario with a uniform PRB utilization of 75% in all cells. Note that the average PRB utilization in the small ISD scenario, shown in Table III, was three times lower (i.e., 24%). For comparison purposes, the results with the original traffic distribution (referred to as 'real traffic') are also reproduced in the figure. It is observed that, as expected, network performance with the initial tilt settings is much worse for the high traffic distribution (red square, OS-uniform high traffic) than for the current traffic distribution (red diamond, OS-real traffic) due to the higher interference levels. Nonetheless, the proposed algorithm achieves performance gains in both figures of merit similar to those obtained with the current (real) traffic distribution. Table VIII compares the performance of OS and last iteration of TF-RET with the new high load conditions.

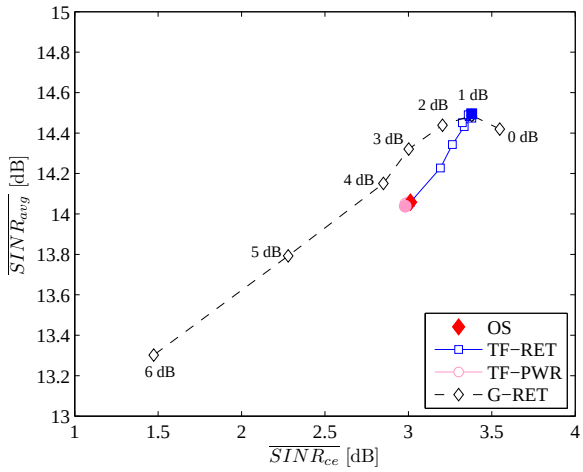

Fig. 6. Performance comparison in large ISD scenario.

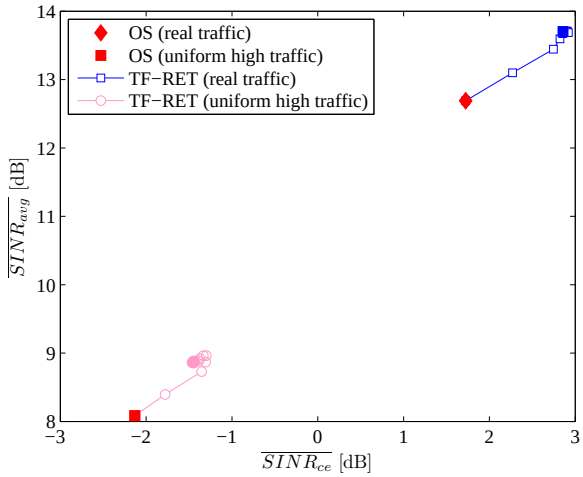

Fig. 7. Algorithm performance under different network loads.

Again, TF-RET outperforms OS with large traffic demand. More specifically, $\overline{SINR_{avg}}$ and $\overline{SINR_{ce}}$ improve by 0.79 and 0.68 dB, respectively. These gains are lower than with the real traffic distribution (1.01 and 1.14 dB, respectively). As a side effect, the average PRB utilization ratio decreases from 75% to 68.83% when TF-RET reaches equilibrium as a result of the increased spectral efficiency.

This article has been accepted for publication in a future issue of this journal, but has not been fully edited. Content may change prior to final publication. Citation information: DOI 10.1109/TVT.2016.2605380, IEEE Transactions on Vehicular Technology

TABLE VII
METHOD PERFORMANCE IN LARGE ISD SCENARIO

	$\overline{SINR_{avg}}$ [dB]	$\overline{SINR_{ce}}$ [dB]	$\overline{UeTHP_{avg}}$ [Mbps]	$\overline{UeTHP_{ce}}$ [Mbps]
OS	14.06	3.01	28.46	9.67
TF-RET	14.50	3.38	29.29	10.16
TF-PWR	14.04	2.98	28.42	9.62
G-RET (3 dB)	14.32	3.00	28.94	9.67

TABLE VIII
METHOD PERFORMANCE WITH HIGH UNIFORM NETWORK LOAD

	OS	TF-RET
$\overline{SINR_{avg}}$ [dB]	8.08	8.87
$\overline{SINR_{ce}}$ [dB]	-2.13	-1.45
Avg. PRB utilization ratio [%]	75	68.83

VI. IMPLEMENTATION ISSUES

A CTR trace processing tool has been developed in Esper [48] to implement the proposed heuristic algorithm in a live network. The time complexity of trace processing is $\mathcal{O}(N_{UE})$, where N_{UE} is the total number of connections collected in the area, while the time complexity of the iterative tuning algorithm is $\mathcal{O}(N_c)$, where N_c is the number of cells in the analyzed area. In practice, execution time is determined by trace processing. To speed up computations, a limited share of connections should be traced per cell. This action is also needed to avoid processor overload and trace storage problems in eNodeBs during the busy hour. Field tests have shown that tracing 20% of connections is enough to obtain robust RSRP and TA estimates. With this setting, the total execution time of the algorithm in a laptop with a clock frequency of 2.6 GHz and 4 GB of RAM is below 1 second per cell and ROP of 15 minutes. The computational load can be reduced by implementing a distributed version of the algorithm, where each cell computes its own tilt parameter changes, provided that the required information is exchanged between nodes.

VII. CONCLUSIONS

In this work, a novel self-tuning algorithm for adjusting remote electrical tilt to solve coverage and interference problems in LTE has been presented. For this purpose, three new indicators have been proposed to detect insufficient cell coverage, cell overshooting and abnormal cell overlapping from connection traces. The proposed heuristic algorithm has been implemented by two fuzzy logic controllers and later tested in a static system-level simulator modeling two realistic scenarios. Results have shown that the proposed method can improve both cell-average and cell-edge SINR values more than 1 dB, thus increasing network spectral efficiency in both small and large ISD scenarios. The proposed method, conceived for network operation, outperforms self-planning methods based on geometric considerations. Note that, although there are more sophisticated self-planning methods, these still rely on propagation and traffic predictions, unlike the self-tuning approach proposed here based on measurements taken from real call traces.

ACKNOWLEDGMENT

This work has been funded by the Spanish Ministry of Economy and Competitiveness (TIN2012-36455 and TEC2015-69982-R) and Optimi-Ericsson and Agencia IDEA (Consejería de Ciencia, Innovación y Empresa, Junta de Andalucía, ref. 59288), co-funded by FEDER.

REFERENCES

[1] NGMN, "Next Generation Mobile Networks Recommendation on SON and O&M Requirements," *Req. Spec. v1*, vol. 23, Dec. 2008.
[2] J.Lempiäinen and M.Manninen, *Radio Interface System Planning for GSM/GPRS/UMTS*. New York, NY, USA: Springer, 2001.
[3] S. Sesia, I. Toufik, and M. Baker, *LTE, the UMTS long term evolution: from theory to practice*. New York, NY, USA: Wiley, 2009.
[4] F. Athley and M. Johansson, "Impact of electrical and mechanical antenna tilt on LTE downlink system performance," in *IEEE 71st Vehicular Technology Conference (VTC 2010-Spring)*, May 2010, pp. 1–5.
[5] G. Wilson, "Electrical downtilt through beam-steering versus mechanical downtilt," in *IEEE 42nd Vehicular Technology Conference*, vol. 1, May 1992, pp. 1–4.
[6] D. Lee and C. Xu, "Mechanical antenna downtilt and its impact on system design," in *IEEE 47th Vehicular Technology Conference*, vol. 2, May 1997, pp. 447–451.
[7] M. Garcia-Lozano and S. Ruiz, "Effects of downtilting on RRM parameters," in *15th IEEE International Symposium on Personal, Indoor and Mobile Radio Communications (PIMRC 2004)*, vol. 3, Sep. 2004, pp. 2166–2170.
[8] I. Forkel, A. Kemper, R. Pabst, and R. Hermans, "The effect of electrical and mechanical antenna down-tilting in UMTS networks," in *3rd International Conference on 3G Mobile Communication Technologies*, May 2002, pp. 86–90.
[9] J. Niemelä, T. Isotalo, and J. Lempiäinen, "Impact of mechanical antenna downtilt on performance of WCDMA cellular network," in *IEEE 59th Vehicular Technology Conference (VTC 2004-Spring)*, vol. 4, May 2004, pp. 2091–2095.
[10] F. Gunnarsson, M. Johansson, A. Furuskar, M. Lundevall, A. Simonsson, C. Tidestav, and M. Blomgren, "Downtilted base station antennas - A simulation model proposal and impact on HSPA and LTE performance," in *IEEE 68th Vehicular Technology Conference (VTC 2008-Fall)*, Sep. 2008, pp. 1–5.
[11] H. Al Hakim, H. Eckhardt, and S. Valentin, "Decoupling antenna height and tilt adaptation in large cellular networks," in *8th International Symposium on Wireless Communication Systems (ISWCS-2011)*, Nov. 2011, pp. 11–15.
[12] D. H. Kim, D. D. Lee, H. J. Kim, and K. C. Whang, "Capacity analysis of macro/microcellular CDMA with power ratio control and tilted antenna," *IEEE Transactions on Vehicular Technology*, vol. 49, no. 1, pp. 34–42, Jan. 2000.
[13] H. Cho, J. K. Kwon, and D. K. Sung, "High reuse efficiency of radio resources in urban microcellular systems," *IEEE Transactions on Vehicular Technology*, vol. 49, no. 5, pp. 1669–1677, Sep. 2000.

This article has been accepted for publication in a future issue of this journal, but has not been fully edited. Content may change prior to final publication. Citation information: DOI 10.1109/TVT.2016.2605380, IEEE Transactions on Vehicular Technology

[14] E. Benner and A. Sesay, "Effects of antenna height, antenna gain, and pattern downtilting for cellular mobile radio," *IEEE Transactions on Vehicular Technology*, vol. 45, no. 2, pp. 217–224, May 1996.

[15] V. Wille, M. Toril, and R. Barco, "Impact of antenna downtilting on network performance in GERAN systems," *IEEE Communications Letters*, vol. 9, no. 7, pp. 598–600, Jul. 2005.

[16] W. Jianhui and Y. Dongfeng, "Antenna downtilt performance in urban environments," in *IEEE Military Communications Conference (MILCOM'96)*, vol. 3, Oct. 1996, pp. 739–744.

[17] J. Niemelä, T. Isotalo, and J. Lempiäinen, "Optimum antenna downtilt angles for macrocellular WCDMA network," *EURASIP Journal on Wireless Communications and Networking*, no. 5, pp. 816–827, Dec. 2005.

[18] I. Siomina, P. Varbrand, and D. Yuan, "Automated optimization of service coverage and base station antenna configuration in UMTS networks," *IEEE Wireless Communications*, vol. 13, no. 6, pp. 16–25, Dec. 2006.

[19] I. Luketic, D. Simunic, and T. Blajic, "Optimization of coverage and capacity of Self-Organizing Network in LTE," in *34th Int. Convention MIPRO*, May 2011, pp. 612–617.

[20] A. Awada, B. Wegmann, I. Viering, and A. Klein, "Optimizing the radio network parameters of the Long Term Evolution system using Taguchi's method," *IEEE Transactions on Vehicular Technology*, vol. 60, no. 8, pp. 3825–3839, Oct. 2011.

[21] V. Bratu and C. Beckman, "Base station antenna tilt for load balancing," in *7th European Conference on Antennas and Propagation (EuCAP)*, Apr. 2013, pp. 2039–2043.

[22] Y. Khan, B. Sayrac, and E. Moulines, "Centralized self-optimization in LTE-A using active antenna systems," in *IFIP Wireless Days*, Nov. 2013, pp. 1–3.

[23] A. Fehske, H. Klessig, J. Voigt, and G. Fettweis, "Concurrent load-aware adjustment of user association and antenna tilts in Self-Organizing Radio Networks," *IEEE Transactions on Vehicular Technology*, vol. 62, no. 5, pp. 1974–1988, Jun. 2013.

[24] G. Hampel, K. Clarkson, J. Hobby, and P. Polakos, "The tradeoff between coverage and capacity in dynamic optimization of 3G cellular networks," in *IEEE 58th Vehicular Technology Conference (VTC 2003-Fall)*, vol. 2, Oct. 2003, pp. 927–932.

[25] B. Hagerman and K. Molnar, "Base station and method for vertical tilt antenna beam sweeping, US Patent 8.682.326," Mar. 25 2014. [Online]. Available: https://www.google.com.tr/patents/US8682326 [accessed Dec. 2015]

[26] M. A. Ismail, X. Xu, and R. Mathar, "Autonomous antenna tilt and power configuration based on CQI for LTE cellular networks," in *10th International Symposium on Wireless Communication Systems (ISWCS 2013)*, Aug. 2013, pp. 1–5.

[27] F. Kasem, A. Haskou, and Z. Dawy, "On antenna parameters self optimization in lte cellular networks," in *3rd International Conference on Communications and Information Technology (ICCIT)*, Jun. 2013, pp. 44–48.

[28] I. Viering and M. Doettling, "Self-optimization of cell overlap, US Patent 8.594.660," Nov. 26 2013. [Online]. Available: https://www.google.es/patents/US8594660 [accessed Dec. 2015]

[29] W. Luo, J. Zeng, X. Su, J. Li, and L. Xiao, "A mathematical model for joint optimization of coverage and capacity in Self-Organizing Network in centralized manner," in *7th International Conference on Communications and Networking in China (CHINACOM)*, Aug. 2012, pp. 622–626.

[30] O. Yilmaz, J. Hamalainen, and S. Hamalainen, "Self-optimization of remote electrical tilt," in *IEEE 21st International Symposium on Personal Indoor and Mobile Radio Communications (PIMRC)*, Sep. 2010, pp. 1128–1132.

[31] H. Eckhardt, S. Klein, and M. Gruber, "Vertical antenna tilt optimization for LTE base stations," in *IEEE 73rd Vehicular Technology Conference*, May 2011, pp. 1–5.

[32] M. Naseer ul Islam and A. Mitschele-Thiel, "Cooperative fuzzy q-learning for self-organized coverage and capacity optimization," in *IEEE 23rd International Symposium on Personal Indoor and Mobile Radio Communications (PIMRC)*, Sep. 2012, pp. 1406–1411.

[33] R. Razavi, S. Klein, and H. Claussen, "Self-optimization of capacity and coverage in LTE networks using a fuzzy reinforcement learning approach," in *IEEE 21st International Symposium on Personal Indoor and Mobile Radio Communications (PIMRC)*, Sep. 2010, pp. 1865–1870.

[34] J. Zhang, C. Sun, Y. Yi, and H. Zhuang, "A hybrid framework for capacity and coverage optimization in Self-Organizing LTE Networks," in *IEEE 24th International Symposium on Personal Indoor and Mobile Radio Communications (PIMRC)*, Sep. 2013, pp. 2919–2923.

[35] A. Thampi, D. Kaleshi, P. Randall, W. Featherstone, and S. Armour, "A sparse sampling algorithm for self-optimisation of coverage in LTE networks," in *International Symposium on Wireless Communication Systems (ISWCS)*, Aug. 2012, pp. 909–913.

[36] J. Chen, H. Jiang, and M. Peng, "Adaptive configuration of antenna down tilt for optimizing coverages in IMT-Advanced systems," in *International Conference on Communication Technology and Application (ICCTA)*, Oct. 2011, pp. 495–499.

[37] S. Berger, M. Soszka, A. Fehske, P. Zanier, I. Viering, and G. Fettweis, "Joint throughput and coverage optimization under sparse system knowledge in LTE-A networks," in *International Conference on ICT Convergence (ICTC)*, Oct. 2013, pp. 105–111.

[38] S. Berger, M. Simsek, A. Fehske, P. Zanier, I. Viering, and G. Fettweis, "Joint Downlink and Uplink Tilt-Based Self-Organization of Coverage and Capacity Under Sparse System Knowledge," in *IEEE Transactions on Vehicular Technology*, no. 99, Oct. 2015.

[39] S. Berger, A. Fehske, P. Zanier, I. Viering, and G. Fettweis, "Comparing Online and Offline SON Solutions for Concurrent Capacity and Coverage Optimization," in *IEEE 80th Vehicular Technology Conference (VTC 20014-Fall)*, Sep. 2014, pp. 1–6.

[40] O. Sallent, J. Perez-Romero, J. Sanchez-Gonzalez, R. Agusti, M. Diaz-Guerra, D. Henche, and D. Paul, "Automatic detection of sub-optimal performance in UMTS networks based on drive-test measurements," in *7th International Conference on Network and Service Management (CNSM)*, Oct. 2011, pp. 1–4.

[41] 3GPP, "Study on minimization of drive-tests in Next Generation Networks," in *TR 36.805, version 9.0.0*, Dec. 2009.

[42] 3GPP, "Subscriber and equipment trace: Trace data definition and management," in *TS 32.423, version 11.7.0*, Mar. 2014.

[43] T. Ross, *Fuzzy logic with engineering applications*. United Kingdom: Wiley, 1995.

[44] M. Miernik, "Application of 2G spatial traffic analysis in the process of 2G and 3G radio network optimization," in *IEEE 65th Vehicular Technology Conference (VTC 2007-Spring)*, Apr. 2007, pp. 909–913.

[45] P. Kyosti *et al.*, "IST-WINNER D1.1.2 WINNER II channel models," 2007. [Online]. Available: http://www.ist-winner.org/WINNER2-Deliverables/D1.1.2v1.1.pdf [accessed Dec. 2015]

[46] COST Action 231, "Digital mobile radio. towards future generation system final report," European Communities, Tech. Rep. EUR 18957, Ch. 4, 1999.

[47] 3GPP, "Radio Frequency (RF) System Scenarios," in *TR 36.942, version 8.2.0*, Jul. 2009.

[48] [Online]. Available: http://www.espertech.com/esper/tutorial.php [accessed Dec. 2015]

Víctor Buenestado received his M.S. degree in Telecommunication Engineering from the University of Málaga, Spain, in 2012. Since 2013, he joined the Communications Engineering Department, University of Málaga, where he is currently working toward the Ph.D. degree in Telecommunications Engineering in a collaborative project with Ericsson. His research interests are focused on self-planning and self-optimization of mobile radio access networks and radio resource management.

Matías Toril received his M.S. in Telecommunication Engineering and Ph.D. degrees from the University of Málaga, Spain, in 1995 and 2007, respectively. Since 1997, he is Lecturer in the Communications Engineering Department, University of Málaga, where he is currently Associate Professor. He has authored more than 90 publications in leading conferences and journals and 3 patents owned by Nokia Corporation. His current research interests include self-organizing networks, radio resource management and graph partitioning.

This article has been accepted for publication in a future issue of this journal, but has not been fully edited. Content may change prior to final publication. Citation information: DOI 10.1109/TVT.2016.2605380, IEEE Transactions on Vehicular Technology

Salvador Luna-Ramírez received his M.S. in Telecommunication Engineering and the Ph.D. degrees from the University of Málaga, Spain, in 2000 and 2010, respectively. Since 2000, he has been with the Department of Communications Engineering, University of Málaga, where he is currently Associate Professor. His research interests include self-optimization of mobile radio access networks and radio resource management.

José María Ruiz-Avilés received his M.S. in Telecommunication Engineering and the Ph.D. degrees from the University of Málaga, Spain, in 2010 and 2015, respectively. From 2008 to 2010, he was with Optimi, first in Málaga, and later in Atlanta, GA, where he worked on mobile network optimization. From 2010 to 2014, he has been with the Communications Engineering Department, University of Málaga, where he worked on radio access network optimization and radio resource management. Since 2014, he joined, as a researcher, in the Ericsson Group. He has been involved in several mobile communication research projects related to self-organizing networks. He also authored a few publications in leading conferences and journals and a few patents owned by Ericsson Group. His current research interests include self-organizing networks and radio resource management.

Adriano Mendo received his M.S. degree in Telecommunication Engineering from the University of Málaga, Spain, in 2004. Since 2004, he joined, as a researcher, Optimi Corporation which became a new member in the Ericsson Group in 2010. He has been involved in several mobile communication research projects related to self-organizing networks. He also authored a few publications in leading conferences and journals and a few patents owned by Ericsson Group. His current research interests include self-organizing networks, radio resource management and customer experience monitoring.